

Kinetic Study of Adsorption of Lead (II) Ions onto Cashew Nut Shells

Chairat Siripatana, Angkana Khuenpetch, Rapeeporn Phromrak,
Wikanda Saengngoen and Kamchai Nuithitikul
Department of Chemical and Process Engineering, Walailak University,
Nakhonsithammarat, 80160 Thai Buri, Thailand

Abstract: Adsorption is an easy, efficient and energy saving method to remove heavy metal ions from water/wastewater. A promising adsorbent needs to be developed from no-cost agricultural/industrial wastes. In this research, cashew nut shells, the waste from a food processing factory were used to adsorb lead ions in aqueous solution. Various initial concentrations of lead were investigated and the adsorption kinetics was determined. Five kinetics models were applied and fitted to the experimental data: pseudo-first-order, pseudo-second-order, Elovich, intraparticle diffusion and liquid film diffusion models. The results showed that the pseudo-second-order model was the best to describe the adsorption of lead ions onto cashew nut shells.

Key words: Adsorption, cashew nut shell, kinetics, lead, saving method

INTRODUCTION

Drastic expansion of process industries in developing countries in the last few decades has generated huge amount of wastewater effluents which contain various pollutants. Among these, heavy metals are considered not only as poisonous substances to various life forms including humans and animals but they also cause a serious environmental problems. Lead is one of the toxic heavy metals found in contaminated wastewater released from several industrial processes such as steel and alloys manufacturing, battery, acid metal plating and finishing, painting and dying processes. The accumulation of lead in the bodies of human and animals could lead to malfunction of nervous system, organs and tissues such as heart, intestines, kidneys and bones. In human, its chronic toxicity occurs at even blood levels of 40-60 µg/dL (Flora *et al.*, 2012) and if not treated could eventually bring about coma and death. Unlike organic pollutants, heavy metals usually change their forms and are not easily degradable. Therefore, it is important to find an efficient method for the removal of lead from this wastewater.

Various techniques have been used to remove heavy metal ions from wastewater such as ion-exchange, chemical precipitation, membrane filtration, reverse osmosis and adsorption. However, many techniques incur high total cost or give low performance and leave chemical residuals as byproducts that require further treatment. In general, adsorption is less expensive and

highly efficient for removing trace amount of heavy metals (Park *et al.*, 2007; Sampranpiboon and Charnkeitkong, 2010; Li *et al.*, 2010). It consumes low energy while being a simple, time-saving and feasible approach. Moreover, many adsorbents can be regenerated and reused. However, commercial adsorbents can be costly. Thus, many researchers have been focusing on the development of efficient adsorbing materials, particularly from no-cost wastes available locally.

Various agricultural and industrial wastes can be used as biosorbents directly or further converted to have better porous structure or their carbon content being activated thus more effective for the removal of lead ions from water (Sampranpiboon and Charnkeitkong, 2010; Li *et al.*, 2010; Dos *et al.*, 2010; Shen *et al.*, 2015). In Thailand, Cashew Nut Shell (CNS) is a locally abundant waste obtained mostly from food processing factories. It is a residual left after extracting cashew nut shell liquid for industrial purposes. To date there have been studies on the removal of dyes from aqueous solution by CNS (Subramaniam and Ponnusamy, 2015). However, this research aims to study the adsorption of lead ions onto CNS. The focus is on the adsorption kinetics and its mechanistic interpretation.

MATERIALS AND METHODS

Raw CNS was locally obtained from a cashew nut factory producing cashew nuts for consumption. The CNS was washed several times, exposed to sun drying

and dried in an oven at 105°C for 24 h before grinding. The ground CNS was sieved with a mesh size of 2.0 mm. The underneath portion was then added with n-hexane in order to remove all cashew nut shell liquid. The remaining solid was finally dried at 105°C for 24 h and kept in desiccator prior to characterization and adsorption studies.

The proximate and ultimate analysis of the prepared CNS was carried out with a thermogravimetric analyzer (TGA 7, Perkin Elmer) and CHNS-O Analyzer (Flash EA1112, Thermo Scientific), respectively.

The adsorption of lead ions (Pb^{2+}) on CNS was studied in a batch operation. Lead nitrate [$\text{Pb}(\text{NO}_3)_2$] was used as the source of Pb^{2+} in the preparation of the aqueous solutions (500 mL) of lead ions. The concentrations of Pb^{2+} were varied between 10-50 mg/L. Then, the aqueous solutions of Pb^{2+} were mixed with 10 g of the CNS adsorbent and placed in a water bath and stirred for a specified contact time. After the contact times were reached at 30°C, the samples were taken and the CNS was rapidly separated using centrifugal method. The concentrations of Pb^{2+} in the clarified supernatant solutions were analyzed with an atomic absorption spectrophotometer (A Analyst 800, Perkin Elmer) based on a prepared calibration curve of the standard solutions. The adsorption capacity of CNS was measured in terms of the amounts of lead ions adsorbed onto CNS per unit mass of CNS at any contact time t , q_t (mg/g) and its equilibrium value, q_e (mg/g). The concentrations of Pb^{2+} in aqueous solutions at the beginning, equilibrium and any time t were assigned as C_0 , C_e and C_t (mg/L), respectively.

RESULTS AND DISCUSSION

The proximate and ultimate analysis results of CNS are shown in Table 1. CNS had high carbon content suggesting the potential of cashew nut shell as a raw material to produce activated carbon. CNS had similar properties to those reported by Kumar *et al.* (2010).

The lead adsorption capacities of CNS when the initial concentrations of Pb^{2+} (C_0) were varied between 10 and 50 mg/L are shown in Fig. 1. The adsorption of Pb^{2+} onto the surface of CNS took place rapidly during the first one minute of contact time. This is due to the greatest number of active sites available at the beginning of the adsorption process. This in turn generates the greatest driving force (the largest concentration gradient of Pb^{2+}). After 1 min, the adsorption rates decreased. This is owing to the less number of active sites on the surface of the CNS which reduces the driving force eventually. At the initial lead concentration of 10 mg/L, the adsorption equilibrium occurred after 240 min and the adsorption

Table 1: Properties of cashew nut shells

Properties	CNS (this study)	CNS ¹¹
Proximate analysis (%)		
Moisture content	5.15	9.83
Volatile matter	69.40	65.21
Ash	1.23	2.75
Fixed carbon	24.22	22.21
Ultimate analysis (%)		
Carbon	44.28	45.21
Hydrogen	6.18	4.25
Nitrogen	0.60	0.21
Oxygen, sulfur and others	48.94	37.75
Moisture		9.83
Ash		2.75

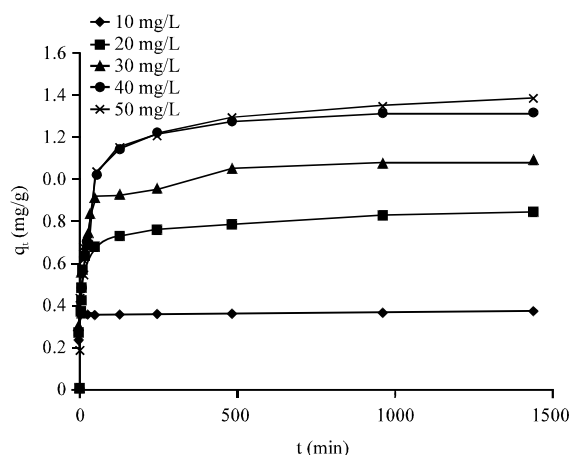


Fig. 1: Adsorption capacities of Pb^{2+} onto CNS at various initial Pb^{2+} concentrations

capacity of 0.37 mg/g was obtained. However, when the initial concentrations of Pb^{2+} were increased from 20-50 mg/L, it took longer time to reach the equilibrium, e.g., 24 h at $C_0 = 50$ mg/L. The equilibrium adsorption capacities were found to be 0.85, 1.08, 1.32 and 1.38 mg/g when C_0 were 20, 30, 40 and 50 mg/L, respectively. It is important to note that the adsorption capacity at $C_0 = 50$ mg/L was similar to that at $C_0 = 40$ mg/L. This suggests that the adsorption process is not solely determined by the mass transfer step. Typically adsorption process consists of three consecutive steps: the adsorbate molecules transfer from bulk solution to the external surface of the adsorbent through the liquid film surrounding the adsorbent surface, the adsorbate molecules diffuse within the adsorbent porous structure and reach its internal surface and the adsorbate molecules attach to the surface atoms of the adsorbent by physical or/and chemical forces. For Pb^{2+} to overcome the mass transfer resistance between aqueous and solid phases, it needs a large driving force provided by a high initial Pb^{2+} concentration. However, at very high initial concentration, the mass transfer resistance becomes lower and thus the attachment step controls the overall process.

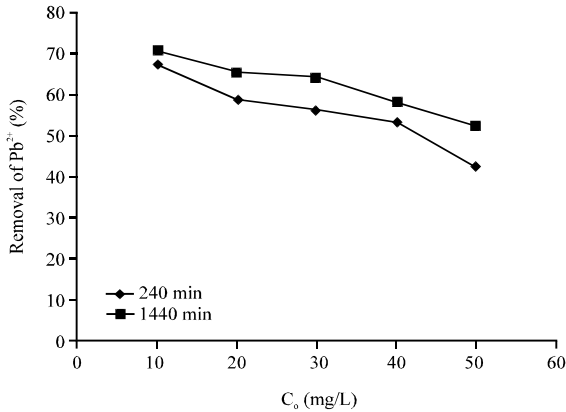


Fig. 2: Percentage Pb^{2+} removal at various initial Pb^{2+} concentrations ($t = 240, 1440$ min)

The effect of initial concentration of Pb^{2+} on percentage removal of Pb^{2+} at 240 and 1440 min is shown in Fig. 2. Removal of Pb^{2+} was defined as $(C_0 - C_t)/C_0 \times 100$. It was found that the percentage Pb^{2+} removal decreased with the increase in initial concentration of Pb^{2+} . At 240 min, the percentage Pb^{2+} removal was 67.13% for 10 mg/L and 41.23% for 50 mg/L of initial concentration, respectively. At 1440 min, the percentage Pb^{2+} removal was 70.63% for 10 mg/L and 52.22% for 50 mg/L of initial concentration. The results are in agreement with previous studies (Kumar *et al.*, 2010; Coelho *et al.*, 2014).

In this research, pseudo-first-order (Lagergren, 1898), pseudo-second-order (Ho and McKay, 1999), Elovich (Aharoni and Tompkins, 1970), intraparticle diffusion and liquid film diffusion (Boyd *et al.*, 1947) models were employed. Pseudo-first-order, pseudo-second-order and Elovich models have been used to explain the adsorption kinetics when the surface adsorption controls the overall process. Intraparticle diffusion and liquid film diffusion models have described the cases when pore diffusion and film diffusion control the overall process, respectively. The pseudo-first-order model is shown in Eq. 1 in which k_1 (min^{-1}) is the rate constant of pseudo-first-order adsorption:

$$\log(q_e - q_t) = \log(q_e) - \frac{k_1}{2.303} t \quad (1)$$

The pseudo-second-order model is presented by Eq. 2 in which k_2 (g/mg/min) is the rate constant of pseudo-second-order adsorption:

$$\frac{t}{q_t} = \frac{1}{k_2 q_e^2} + \frac{1}{q_e} t \quad (2)$$

The Elovich model is shown in Eq. 3 where α (mg/g/min) is the initial adsorption rate and β (g/mg) is the desorption coefficient. The model is satisfied in chemical adsorption processes and assumes the adsorbent surfaces are energetically heterogeneous (Figaro *et al.*, 2009):

$$q_t = \frac{1}{\beta} \ln(\alpha\beta) + \frac{1}{\beta} \ln(t) \quad (3)$$

The intraparticle diffusion model is shown in Eq. 4 in which k_{int} ($\text{mg/g/min}^{0.5}$) is the intraparticle diffusion rate coefficient and C is a constant relevant to the thickness of the boundary layer:

$$q_t = k_{\text{int}} t^{0.5} + C \quad (4)$$

The liquid film diffusion model is represented by Eq. 5 in which k_{fd} (min^{-1}) is the film diffusion rate coefficient:

$$-\ln\left(1 - \frac{q_t}{q_e}\right) = k_{\text{fd}} t \quad (5)$$

The plots of the experimental data according to the five models at various initial Pb^{2+} concentrations are shown in Fig. 3. The pseudo-second-order model best fitted to the experimental data as confirmed by the coefficients of determination (R^2). All kinetic parameters were evaluated and summarized in Table 2. The values of q_e calculated from pseudo-second-order model were closer to the experimental values than those from pseudo-first-order model. This implied that a chemo-sorption which involves the sharing of valence forces or electron exchange between Pb^{2+} and CNS controls the overall process. Since, the intercepts of the plots between q_t and $t^{0.5}$ did not pass through the origin, intraparticle diffusion is not solely the controlling step. This means that the overall process is controlled not only by surface adsorption but also by intraparticle diffusion. We therefore employed more elaborate model based on diffusion theory to get more insight as following.

For isothermal single component adsorption system with parallel pore and surface diffusion (Worch, 2012) the mass balance around a thin shell element in the particle is represented by Eq. 6:

$$\begin{aligned} \epsilon \frac{\partial q}{\partial t} + (1 - \epsilon) \frac{\partial q_{\mu}}{\partial t} = \epsilon D_p \frac{1}{r^s} \frac{\partial}{\partial r} \left(r^s \frac{\partial q}{\partial r} \right) + \\ (1 - \epsilon) D_s \frac{1}{r^s} \frac{\partial}{\partial r} \left(r^s \frac{\partial q_{\mu}}{\partial r} \right) \end{aligned} \quad (6)$$

Table 2: Adsorption kinetic parameters of CNS at various C_0 based on pseudo-first-order, pseudo-second-order, Elovich, intraparticle diffusion and liquid film diffusion models

C_0 (mg/L)	Pseudo-first-order			Pseudo-second-order			Elovich		Intraparticle diffusion			Liquid film diffusion	
	k_1 (min^{-1})	Cal. q_e (mg/g)	R^2	k_2 (g/mg/min)	Cal. q_e (mg/g)	R^2	α (g/mg/min)	β (mg/g)	R^2	K_{int} ($\text{mg/g/min}^{0.5}$)	R^2	k_{fl} ($\text{min}^{0.5}$)	R^2
10	0.023	0.069	0.440	5.517	0.362	0.999	23.92	27.25	0.803	0.018	0.525	0.024	0.440
20	0.022	0.466	0.692	0.362	0.732	0.992	0.770	8.31	0.906	0.070	0.842	0.022	0.692
30	0.027	0.713	0.934	0.160	0.996	0.983	0.693	6.27	0.944	0.096	0.949	0.027	0.934
40	0.019	0.891	0.955	0.134	1.086	0.971	1.759	7.35	0.824	0.089	0.978	0.019	0.994
50	0.019	1.066	0.909	0.085	1.149	0.959	0.391	4.83	0.951	0.121	0.901	0.019	0.909

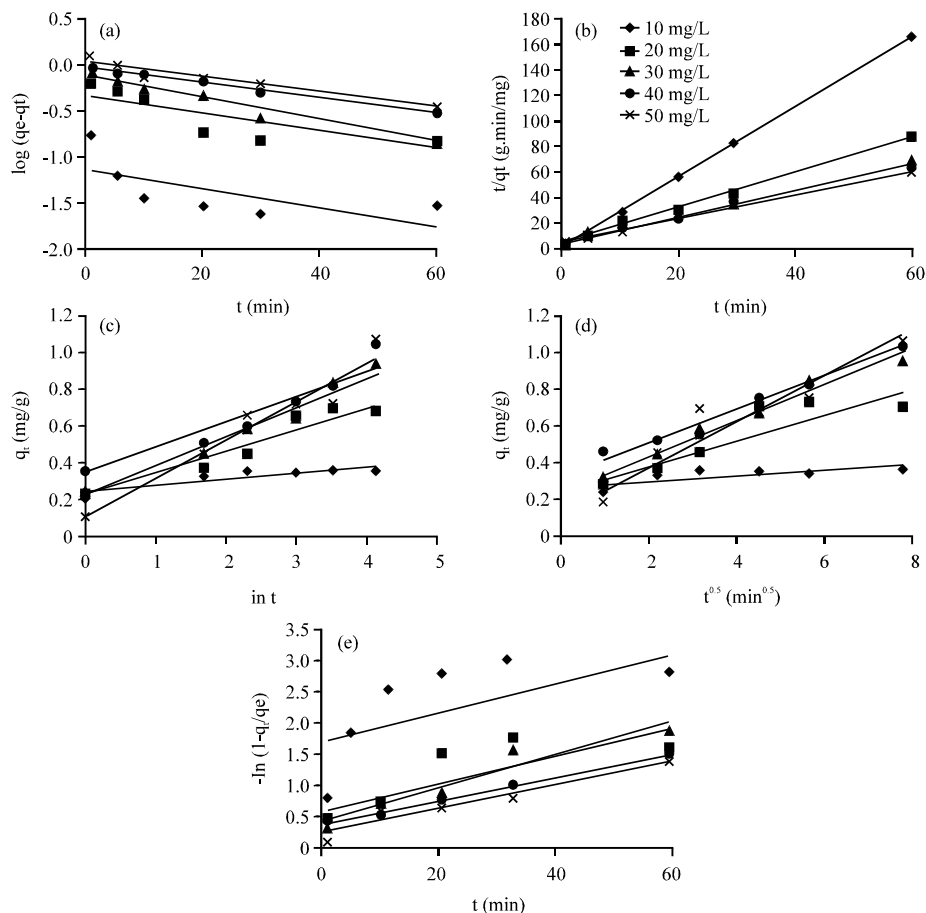


Fig. 3: Adsorption of Pb^{2+} onto CNS at various C_0 according to: a) pseudo-first-order model; b) pseudo-second-order model; c) Elovich model; d) intraparticle diffusion model and e) liquid film diffusion model

Where:

q and q_{μ} = Concentrations in pore and in the adsorbed phase

ϵ = The voidage of the particle

s = The particle shape factor

r = The radius of particle

D_s and D_p = Surface and pore diffusivities

$$\frac{\partial q}{\partial t} = D_{app} \nabla^2 q \quad (7)$$

$$D_{app} = \frac{\epsilon D_p + (1 - \epsilon) K D_s}{\epsilon + (1 - \epsilon) K} \quad (8)$$

With the assumptions of local equilibrium and linear isotherm, the Fickian diffusion (Eq. 7) was obtained. The apparent diffusivity, D_{app} was calculated from Eq. 8 in which K was the Henry constant:

When Eq. 7 was solved analytically (Rittirut *et al.*, 2010) and plotted against the experimental data (Fig. 4), a good agreement between the experimental data and the combined pore-surface adsorption model was obtained during the initial time up to a few minutes for all initial Pb^{2+}

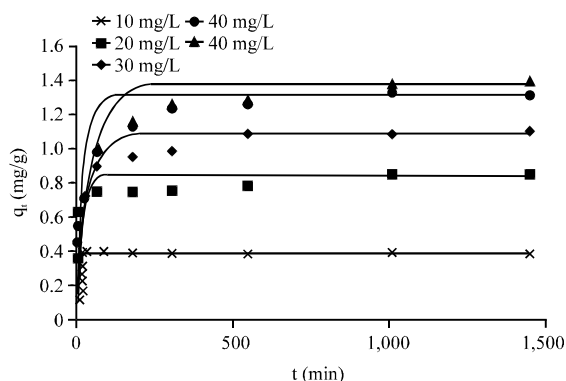


Fig. 4: The comparison between the prediction and experimental data for adsorption capacities at various initial Pb^{2+} concentrations; dots for experimental data line for modeling

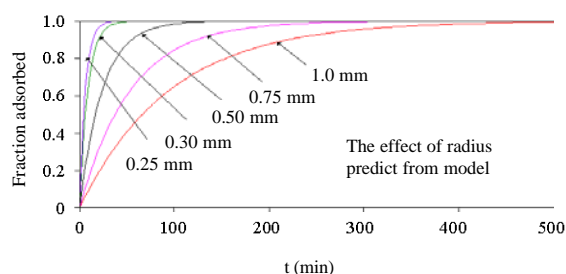


Fig. 5: The prediction effect of adsorbent radius on the adsorption kinetics at $C_0 = 40$ mg/L

concentrations. The model then started to over-predict the extent of adsorption at longer times. This is not a surprise because linear isotherm could represent the current system poorly. All predictions would be much better for longer time if Langmuir isotherm was used instead of the linear one. However, the model is good enough to explain the trends of the adsorption curves in terms of fundamental variables and parameters. If better prediction is required, we can use Langmuir isotherm. However, in this case some elaborated numerical methods are required.

Figure 5 shows the effect of particle size on the adsorption kinetics. The model predicted that the smaller the particles, the higher the adsorption rate. This is true to a certain limit but if the particle is too small, the rate might go in the opposite direction since the particles tend to clump together and create mass transfer barriers. However, this prediction needs further experimental verification.

CONCLUSION

The adsorption kinetics of Pb^{2+} in aqueous solution onto cashew nut shells followed pseudo-second-order

model. The adsorption process occurred rapidly during the first one minute of contact time. When the initial concentration of Pb^{2+} in aqueous solution was increased, the adsorption capacity increased but became constant at 40 mg/L. However, the percentage Pb^{2+} removal decreased with the initial concentration of Pb^{2+} .

ACKNOWLEDGEMENT

This research was financially supported by Institute of Research and Development, Walailak University.

REFERENCES

- Aharoni, C. and F.C. Tompkins, 1970. Kinetics of adsorption and desorption and the elovich equation. *Adv. Catal.*, 21: 1-47.
- Boyd, G.E., A.W. Adamson and L.S. Jr. Myers, 1947. The exchange adsorption of ions from aqueous solutions by organic zeolites II Kinetics. *J. Am. Chem. Soc.*, 69: 2836-2848.
- Coelho, G.F., J.A.C. Goncalves, C.R.T. Tarley, J. Casarin and H. Nacke *et al.*, 2014. Removal of metal ions Cd (II), Pb (II) and Cr (III) from water by the cashew nut shell *Anacardium occidentale* L. *Ecol. Eng.*, 73: 514-525.
- Dos, S.V.C.G., C.R.T. Tarley, J. Caetano and D.C. Dragunski, 2010. Assessment of chemically modified sugarcane bagasse for lead adsorption from aqueous medium. *Water Sci. Technol.*, 62: 457-465.
- Figaro, S., J.P. Avril, F. Brouers, A. Ouensanga and S. Gaspard, 2009. Adsorption studies of molasses wastewaters on activated carbon: Modelling with a new fractal kinetic equation and evaluation of kinetic models. *J. Hazard. Mater.*, 161: 649-656.
- Flora, G., D. Gupta and A. Tiwari, 2012. Toxicity of lead: A review with recent updates. *Interdiscip. Toxicol.*, 5: 47-58.
- Ho, Y.S. and G. McKay, 1999. Pseudo-second order model for sorption processes. *Process. Biochem.*, 34: 451-465.
- Kumar, P.S., S. Ramalingam, C. Senthamarai, M. Niranjana and P. Vijayalakshmi *et al.*, 2010. Adsorption of dye from aqueous solution by cashew nut shell: Studies on equilibrium isotherm, kinetics and thermodynamics of interactions. *Desalin.*, 261: 52-60.
- Lagergren, S., 1898. About the theory of so-called adsorption of soluble substances. *Kungliga Svenska Vetenskapsakademiens Handlingar*, 24: 1-39.
- Li, Y., Q. Du, X. Wang, P. Zhang and D. Wang *et al.*, 2010. Removal of lead from aqueous solution by activated carbon prepared from *Enteromorpha prolifera* by zinc chloride activation. *J. Hazard. Mater.*, 183: 583-589.

- Park, H.G., T.W. Kim, M.Y. Chae and I.K. Yoo, 2007. Activated carbon-containing alginate adsorbent for the simultaneous removal of heavy metals and toxic organics. *Process Biochem.*, 42: 1371-1377.
- Rittirut, W., C. Thongurai and C. Siripatana, 2010. Mathematical simulation of solid-liquid diffusion in continuous countercurrent extraction process, Part I-modeling development. *Int. J. Chem. Reactor Eng.*, Vol. 8,
- Sampranpiboon, P. and P. Charnkeitkong, 2010. Equilibrium isotherm, thermodynamic and kinetic studies of lead adsorption onto pineapple and paper waste sludges. *Int. J. Energy Environ.*, 4: 89-93.
- Shen, Z., F. Jin, F. Wang, O. McMillan and A.A. Tabbaa, 2015. Sorption of lead by Salisbury biochar produced from British broadleaf hardwood. *Bioresour. Technol.*, 193: 553-556.
- Subramaniam, R. and S.K. Ponnusamy, 2015. Novel adsorbent from agricultural waste for methylene blue dye removal: Optimization by response surface methodology. *Water Resour. Ind.*, 11: 64-70.
- Worch, E., 2012. *Adsorption Technology in Water Treatment: Fundamentals, Processes and Modeling*. Walter de Gruyter GmbH & Co. KG, Berlin, Germany, ISBN-13: 9783110240238, Pages: 344.